International Journal of Biological Macromolecules 183 (2021) 1174–1183

Contents lists available at ScienceDirect

International Journal of Biological Macromolecules

journal homepage: http://www.elsevier.com/locate/ijbiomac

Prolonged release and shelf-life of anticoagulant sulfated polysaccharides encapsulated with ZIF-8

Jie Zheng [a,1], Bingzhi Li [b,1], Yuan Ji [b], Yin Chen [c,*], Xun Lv [d,*], Xing Zhang [b,*], Robert J. Linhardt [e]

[a] College of Biotechnology and Pharmaceutical Engineering, Nanjing Tech University, Nanjing 211816, China
[b] School of Food Science and Pharmaceutical Engineering, Nanjing Normal University, Nanjing 210023, China
[c] College of Food and Pharmacy, Zhejiang Ocean University, 1 South Haida Road, Zhoushan 316000, China
[d] CAS Key Laboratory of Pathogenic Microbiology and Immunology, Institute of Microbiology, Chinese Academy of Sciences (CAS), Chaoyang District, Beijing 100101, China
[e] Department of Chemistry and Chemical Biology, Center for Biotechnology and Interdisciplinary Studies, Rensselaer Polytechnic Institute, Troy, NY, 12180, USA

ARTICLE INFO

Article history:
Received 4 February 2021
Received in revised form 10 April 2021
Accepted 2 May 2021
Available online 10 May 2021

Keywords:
Metal-organic frameworks
ZIF-8
Anticoagulant
Sulfated polysaccharides
Hyaluronic acid

ABSTRACT

Natural active polysaccharides are attracting increased attention from pharmaceutical industries for their valuable biological activities. However, the application of polysaccharides has been restricted due to their relatively large molecular weight, complex structure, and instability. Metal-organic frameworks (MOFs) have emerged to help deliver cargo to specific locations, achieving the objectives of eliminating the potential damage to the body, protecting the drugs, and improving therapeutic effectiveness. Here, a pH-responsive zeolitic imidazolate framework (ZIF-8) was synthesized to encapsulated three sulfated polysaccharides (heparin, fucan sulfate, fucosylated chondroitin sulfate) and a non-sulfated polysaccharide, hyaluronic acid. The resulting polysaccharides@ZIF-8 biocomposites showed differences in terms of morphology, particle size, encapsulation, and release efficiency. These biocomposites retained antithrombotic activity and the framework ZIF-8 effectively protected these polysaccharides from degradation and prolonged shelf-life of the anticoagulants from the unfavorable environment.

1. Introduction

Sulfated polysaccharides, extracted from natural resources or obtained by modifying the sugar chain with sulfates [1], possess multiple functions, such as immunoregulation [2], anti-tumor [3], antioxidative [4], antithrombotic [5], and anti-virus activities [6], and are widely used as anticoagulant drugs. For example, heparin (HP), consisting of the alternating uronic acid residues (L-iduronic (IdoA) or D-glucuronic acid (GlcA)) and *N*-acetyl-D-glucosamine, is a drug approved by the U.S. Food and Drug Administration (FDA) and has been applied in the prevention and treatment of deep venous thrombosis and other coagulation abnormalities [7]. However, the anionic nature of heparin can result in strong interactions with critical proteins, leading to substantial side effects. In addition to a lack of specificity, heparin suffers from low tissue permeability, short serum half-life and poor oral absorption, and low stability [8–11]. Due to the drawbacks of heparin, a series of new sulfated polysaccharides have been investigated that show great potential as a new generation anticoagulants. For example, fucan sulfate (FuS), sulfated polysaccharide composed mainly of fucose, and fucosylated chondroitin sulfate (FCS), bearing three parts of uronic acid, amino sugar and fucose side chain, display promising anticoagulant activity and oral efficacy and exhibit a different anticoagulant mechanism from that of heparin derivatives, and show decreased risks of adverse effects [12–15]. The poor dosage control of sulfated polysaccharides can still lead to either fast clearance from the body (under-dosage) or spontaneous hemorrhage (over-dosage). Besides, in FCS, the sulfated fucose branch is the most important pharmacophore and it can be readily cleaved resulting in loss of potency [16]. Therefore, developing a delivery system that not only protects sulfated polysaccharides but also acts as a molecular transport to release the encapsulated biomolecules in a controlled way is highly desirable.

Carriers for polysaccharides was shown to protect them from environments that typically lead to their degradation, to act as a gate for molecular transport, and to release the encapsulated biomolecules under controlled conditions, such as graphene [17], Fe_3O_4 [18], silica [19], hydrogels [20] and polymer film materials [21]. However, some conventional supports are not finely tunable and crystalline which leads to low loading efficiency, low stability, and/or biomacromolecules leaching. Metal-organic frameworks (MOFs), constructed by the coordination between metal ions and organic ligands, are a series of porous crystals that have emerged as excellent carriers for biomacromolecules (e.g. protein, DNA, antibiotics, and polysaccharides) because of tunable pore size, high surface area, and versatile framework composition [22–24]. MOFs

* Corresponding author.
E-mail addresses: mojojo1984@163.com (Y. Chen), wslvxun@163.com (X. Lv), zhangxing@njnu.edu.cn (X. Zhang).
[1] J.Z. and B.L. contributed equally.

https://doi.org/10.1016/j.ijbiomac.2021.05.007
0141-8130/

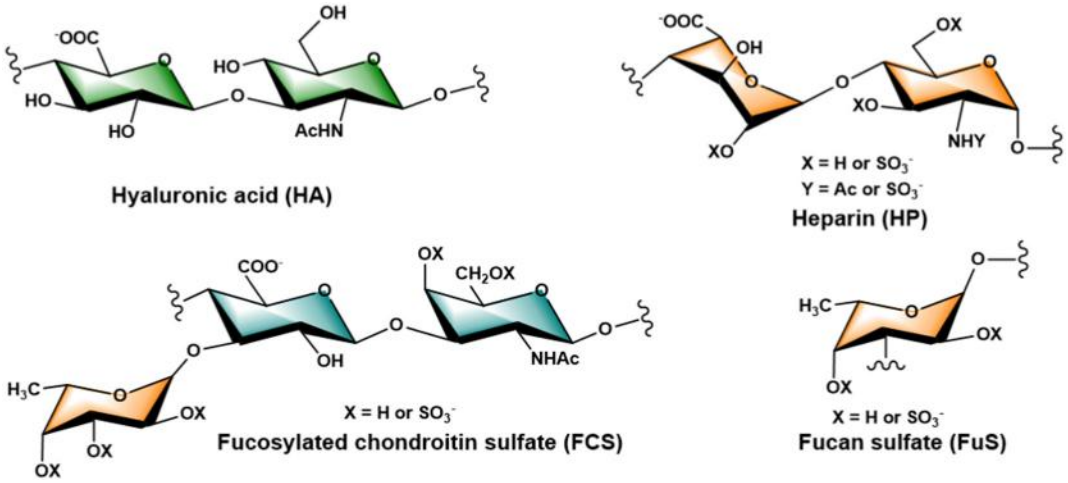

Fig. 1. The general structures of heparin, hyaluronan, fucosylated chondroitin sulfate, and fucan sulfate.

with the larger surface area and tunable porosity properties enable the loading of more biomacromolecules than conventional carrier materials, and the shielding effect and biocompatibility of the MOFs allow the stabilization of the conformational structure of the biomacromolecules, thus maintaining their stability and activity [25,26]. Besides, studies have demonstrated that negatively charged molecules trigger the growth of MOFs since the electrostatic interactions between biomolecules and metal ions and increased local concentrations of metal ions on the surface of the biomolecule trigger the self-assembly of the framework. Zeolitic imidazolate frameworks (ZIF-8), one typical material in the MOFs family being successfully employed to encapsulate biomacromolecules is feasible, affording good biocompatibility, mild preparation conditions, and pH responsiveness [27]. Therefore, as part of our ongoing work on biological studies of sulfated polysaccharides, in this study, we have focused on sulfated polysaccharides (HP, FuS, FCS) with anticoagulant activity and a non-sulfated polysaccharide, hyaluronic acid (HA) (Fig. 1) [28]. The encapsulation efficiencies and therapeutic release profiles of each polysaccharides@ZIF-8 biocomposite were assessed. In addition, the anticoagulant activity and the tolerance for unfavorable environmental conditions were investigated for these biocomposites (Scheme 1).

2. Materials and methods

2.1. Materials

Hyaluronic acid (HA) was purchased from MACKLIN (Shanghai, China). Heparin sodium salt (HP) from porcine intestinal mucosa was purchased from Sangon Biotech (Shanghai, China). Fucose sulfate (FuS) and fucosylated chondroitin sulfate (FCS) polysaccharides were prepared in our lab [29]. $Zn(OAc)_2 \cdot 2H_2O$ and $Zn(NO_3)_2 \cdot 6H_2O$ were purchased from HUSHI (Shanghai, China). Fluorescein isothiocyanate

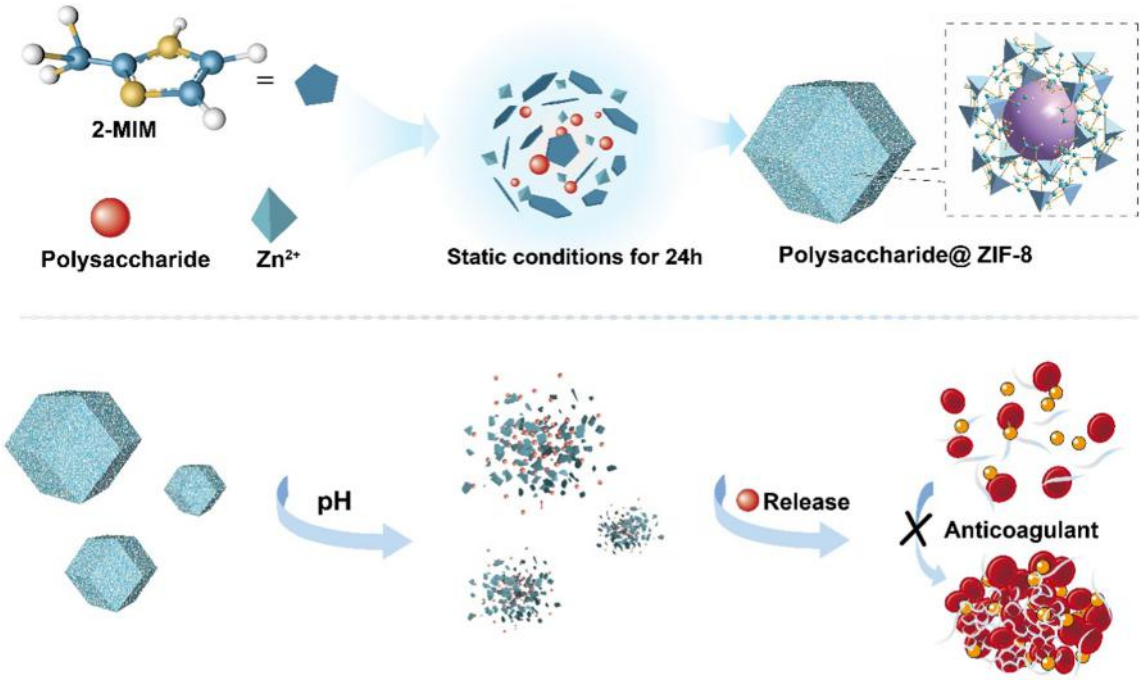

Scheme 1. Schematic representation of the synthesis of polysaccharides@ZIF-8 biocomposites.

(FITC) and 2-methylimidazole (2-MIM) were purchased from Aladdin (Shanghai, China). An activated partial thromboplastin time (APTT) kit was purchased from Leagene Biotechnology (Beijing, China). Rabbit plasma was purchased from Hopebio (Qingdao, China). All other chemicals were of reagent grade and obtained commercially.

2.2. Synthesis of polysaccharides@ZIF-8 biocomposites

The synthesis of polysaccharides@ZIF-8 biocomposites were carried out using a metal (M) to ligand (L) ratio M:L = 1:4 and 1:20 (M = Zn $(OAc)_2 \cdot 2H_2O$ and $Zn(NO_3)_2 \cdot 6H_2O$, L = 2-MIM; respectively). The final concentration of the corresponding polysaccharide was 0.36 $mg \cdot mL^{-1}$. The stock solution of the corresponding precursors Zn $(OAc)_2 \cdot 2H_2O$ (80 mM), $Zn(NO_3)_2 \cdot 6H_2O$ (80 mM), 2-methylimidazole (2-MIM; 457.1 mM, 2285.7 mM), and polysaccharides (2.4 $mg \cdot mL^{-1}$) were prepared in DI water at room temperature. Then, 700 μL of the 2-MIM solution was premixed with 300 μL of polysaccharides solution, followed by the addition of 1 mL of Zn^{2+} solution. The resulting solutions were left standing at room temperature for 24 h. Afterward, the solids were collected by centrifugation and washed with deionized water. The solids were then air-dried at room temperature.

2.3. Characterization

The chemical structure of the samples was assessed using a VECTOR-22 Fourier transform infrared (FTIR) spectroscope (Bruker Corp., Germany) in the wavenumber range of 400–4000 cm^{-1}. The crystalline structure of the samples was determined using 3 kW X-ray diffractometer (XRD) with a Cu Kα radiation source (Rigaku Smartlab, Japan). The sample was scanned with diffraction angles of 5–50° (2θ) at a scanning rate of 10°/min. The morphology of samples was analyzed utilizing HITACHI SU8100 high-resolution field emission scanning electron microscope (SEM). The confocal laser scanning microscopy (CLSM) data were recorded by Olympus FV3000 microscope, with excitation at 640 nm and emission at 650–675 nm.

2.4. The encapsulation efficiency of polysaccharides@ZIF-8

The encapsulation efficiency (EE%) of each polysaccharides@ZIF-8 was assessed using UV–vis spectroscopy by the carbazole and phenol-sulfuric acid assay, which is a direct method to quantify polysaccharides by colorimetry (vide infra).

$$EE\%(HP) = \frac{A + 0.0411}{2.6157 * 0.36}$$

$$EE\%(HA) = \frac{A - 0.1038}{2.95 * 0.36}$$

$$EE\%(FuS) = \frac{A + 0.1108}{0.3713 * 0.36}$$

$$EE\%(FCS) = \frac{A + 0.0268}{0.5191 * 0.36}$$

A: the absorbance of polysaccharides.

2.5. Release test of polysaccharides@ZIF-8

The polysaccharides@ZIF-8 were added to 2 mL of phosphate buffer (NaH_2PO_4 and Na_2HPO_4), and the sample was kept under stirring. Aliquots of 200 μL of the supernatant were collected by centrifugation (4427*g*, 3 min) and replaced with the same volume of fresh buffer. The amount of polysaccharides released in the incubation media was determined by carbazole and phenol-sulfuric acid assay.

2.6. In vitro anticoagulant activity assay

The clot formation was determined spectrophotometrically at a wavelength of 500 nm. Based on the data, a time course of thrombus formation was made. The activated partial thromboplastin time (APTT) kit and standard rabbit plasma were used as previously described [30].

2.7. Carbazole and phenol-sulfuric acid assay

The carbazole assay was reported previously [31]. Ammonium sulfamate (20 μL, 4 M) and 200 μL samples were mixed for 1 min. Then, sodium tetraborate (1 mL, 25 mM) in sulfuric acid was added and mixed carefully. The mixture was heated at 100 °C for 5 min and cooled to room temperature. Afterward, carbazole solution (40 μL, 0.1%) was added and the resulting mixture was heated again at 100 °C for 15 min and then cooled down to room temperature. Finally, UV–*vis* spectroscopy was used to analyze the resultant solution at 520 nm.

The phenol-sulfuric acid method was based on the Dubis' et al. method [32]. Phenol solution (80 μL of 5% (*w*/*v*)) was mixed with 200 μL of samples. Then, concentrated sulfuric acid (1 mL) was added and the mixture was heated in a boiling water bath for 20 min and then cooled in an ice bath. The light absorption at 490 nm was measured on the spectrophotometer.

3. Results and discussion

3.1. Optimization of reaction conditions

We first investigated the different zinc precursors and varying metal to ligand ratio to the loading capacity and release properties of the biocomposites derived from the ZIF-8 systems. The synthesis of HP@ZIF-8 was performed by different zinc precursors ($Zn(OAc)_2 \cdot 2H_2O$ and $Zn(NO_3)_2 \cdot 6H_2O$) and varying metal to ligand ratio (M:L = 1:4 and 1:20). Fig. 2 showed the SEM images and XRD patterns of the ZIF-8 synthesized using different zinc precursors at variable Zn/2-MIM ratios. When using $Zn(OAc)_2$ as zinc precursor, it was found that all resulting products exhibited a 2D layered structure at the molar ratios of 1:4 (Fig. 2a). The XRD pattern of ZIF-8 agreed with typical monoclinic (*dia*) structure and that of HP@ZIF-8 was similar *kat* structure (Fig. 2d) [33]. Previous study has reported that layered structure could be an intermediate form of ZIF-8 crystals [2,34]. The consequence could result from decreasing the amount of deprotonated linkers at a low 2-MIM concentration, which limits the rate of phase transformation [35]. The typical ZIF-8 particles with rhombic dodecahedron shape were obtained from $Zn(OAc)_2$ at the molar ratios of 1:20 (Fig. 2b). The prominent reflections at 2θ = 7.205°, 12.643°, and 17.943° were observed clearly, which are in good agreement with simulated patterns of ZIF-8 single crystal with typical *sod* structure (Fig. 2e). When $Zn(NO_3)_2$ was used, the particles prepared at the molar ratio of 1:20 showed bumpy surfaces, which proved the different zinc precursors could also affect the morphology and crystalline phase of the product (Fig. 2c). The X-ray diffraction patterns collected for composites indicated that four polysaccharides@ZIF-8 at the molar ratios of 1:20 had strong diffraction peaks being in good agreement with simulated patterns of ZIF-8 single crystal with typical *sod* structure, confirming that the encapsulation of polysaccharides caused no significant influence on the crystal structure of ZIF-8.

The data showed that for HP@ZIF-8 biocomposite, the encapsulation efficiencies were less than 80% using $Zn(OAc)_2 \cdot 2H_2O$ and metal to ligand ratios of 1:4 and 1:20 (Fig. 3a). With respect to release behavior from as-prepared HP@ZIF-8, we carried out the controlled drug-release test, as recorded in Fig. 3b and c. In neutral (pH 7.4) and acidic (pH 5.6) buffer solution, the encapsulated heparin released quickly in 20 min, showing that as-prepared HP@ZIF-8 had undesirable stability in the neutral and acidic environment. The higher EE% values (>95%) were observed for samples obtained from the $Zn(NO_3)_2 \cdot 6H_2O$, for 1:20 M:L ratios (Fig. 3a). In buffer (pH 7.4), there was less than 20% of

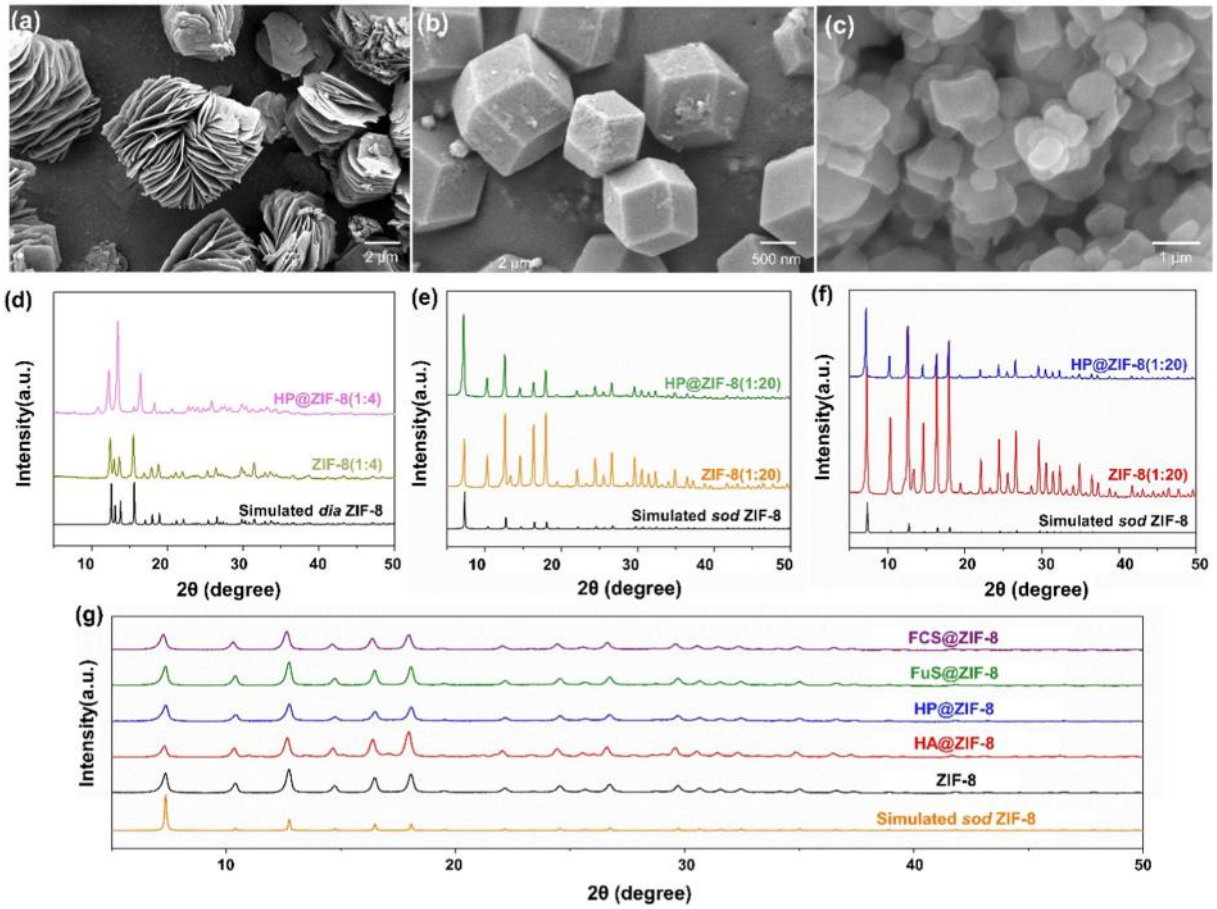

Fig. 2. SEM images of HP@ZIF-8 (a) M(OAc^-): L = 1:4; (b) M(OAc^-): L = 1:20; (c) M(NO_3^-): L = 1:20. XRD patterns of HP@ZIF-8 (d) M(OAc^-): L = 1:4; (e) M(OAc^-): L = 1:20; (f) M (NO_3^-): L = 1:20. (g) XRD patterns of ZIF-8, HA@ZIF-8, HP@ZIF-8, FuS@ZIF-8 and FCS@ZIF-8.

heparin been released within 3 h, while in the presence of an acidic environment, the release amount of heparin was up to 45% within 3 h (Fig. 3d). These results suggested that the ZIF-8 obtained by this synthetic condition could be a good choice for loading heparin and could enable pH-triggered drug release. Therefore, in subsequent experiments, We adopted $Zn(NO_3)_2 \cdot 6H_2O$ precursors at M: L ratios 1:20.

3.2. Characterization of polysaccharides@ZIF-8 biocomposites

The samples were washed with water and ethanol to ensure the complete removal of polysaccharides loosely attached to the particle surface to ascertain the synthesis of polysaccharides@ZIF-8. The collected solids were analyzed by Fourier transform infrared spectroscopy (FTIR) (Fig. S1). The vibrational mode at 421 cm^{-1}, found in all samples, is assigned to the Zn—N stretching mode and thus confirms the networks are composed of 2-MIM connected via Zn nodes. The strong peak at 1584 cm^{-1} and 3135 cm^{-1} could be attributed to the stretching of C═N, and imidazole C—H stretching, respectively [36]. For each polysaccharide used, additional bands originating from the specific pendant groups were observed. 1615 and 1407 cm^{-1} are the antisymmetric and symmetrical stretching vibration peaks of the carboxyl group, and 1373 cm^{-1} was the characteristic absorption peak of sugar (amide) in HA [37]. In addition, the β-glycosidic bond at 891 cm^{-1} and N—H bonds at 1662 $cm^{-1}$was detected in HP. The C-O-C stretching vibration of pyran ring was at 1025 $cm^{-1}$for FuS [38], and the characteristic absorption peak of C—N in acetamide at 1560 cm^{-1} and O-C═O at 1378 cm^{-1} disappeared in FCS@ZIF-8, which may be caused by the combination of FCS and ZIF-8 [39]. Finally, those biocomposites obtained from sulfated biomacromolecules (HP, FCS, and FuS) present additional weak vibrational bands at 1220–1240 cm^{-1} (S═O) which indicated the successful synthesis of polysaccharides@ZIF-8 biocomposites (Fig. 4).

The morphology of the control samples of ZIF-8 and the corresponding polysaccharides@ZIF-8 were assessed by scanning electron microscopy (SEM) (Fig. 5a–e). The micrographs obtained from all samples show the formation of the characteristic rhombic dodecahedron morphology. The dried solids were analyzed by X-ray diffraction. All crystals had strong diffraction peaks at 2- Theta of 7.205°, 10.285°, 12.643°, 14.602°, 16.354°, and 17.943°, and the prominent peaks corresponding to planes (0 1 1), (0 0 2), (1 1 2), (0 2 2), (0 1 3) and (2 2 2) were identical with previous reports, confirming the typical sodalite structure of four types polysaccharides@ZIF-8 [40,41]. The X-ray diffraction patterns collected for composites was in good agreement with simulated patterns of ZIF-8 single crystal indicated that the crystal structure of ZIF-8 was not significantly affected after the encapsulation of polysaccharides. According to the data of DLS (Fig. S2), polysaccharides@ZIF-8 exhibited a wide hydrodynamic diameter distribution with an average size of 1315 nm (HA@ZIF-8), 2227 nm (HP@ZIF-8), 1610 nm (FuS@ZIF-8), and 3348 nm (FCS@ZIF-8), which were slightly increased compared to naked ZIF-8 (1015 nm). The reason could be the differences in the molecular weight and electronegativity of polysaccharides, and the agglomeration of polysaccharides@ZIF-8. To further confirm that the polysaccharides were encapsulated in the ZIF-8 particles, fluorescein isothiocyanate (FITC) labeled hyaluronic acid was used in the synthesis of the ZIF-8 particles, and the resultant biocomposite was characterized by confocal laser scanning microscopy (CLSM) (Fig. 5f). CLSM images revealed a homogeneous distribution of fluorescent emission across ZIF-8 particles, and the polysaccharides predominantly localized towards the internal region of crystalline particles, suggesting that

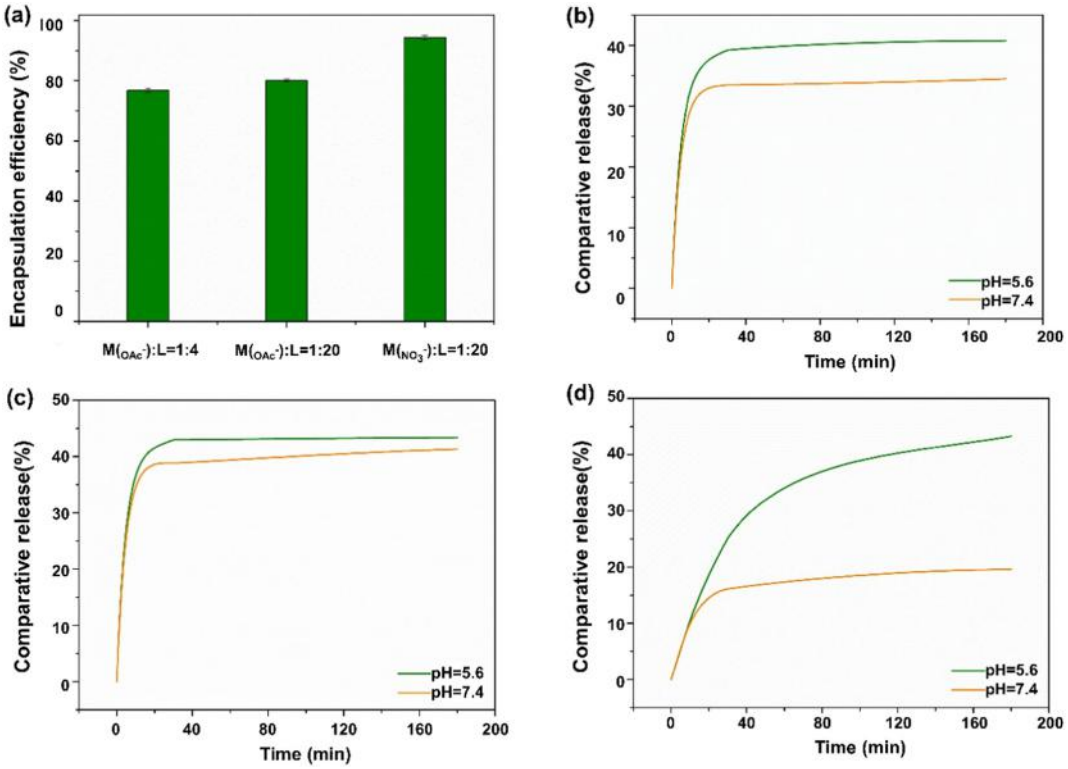

Fig. 3. (a) The encapsulation efficiency of the HP@ZIF-8 synthesized by different zinc precursors and varying metal to ligand ratio. Release profiles of HP@ZIF-8 (b) M(OAc^-): L = 1:4; (d) M(OAc^-): L = 1:20; (f) M(NO_3^-): L = 1:20.

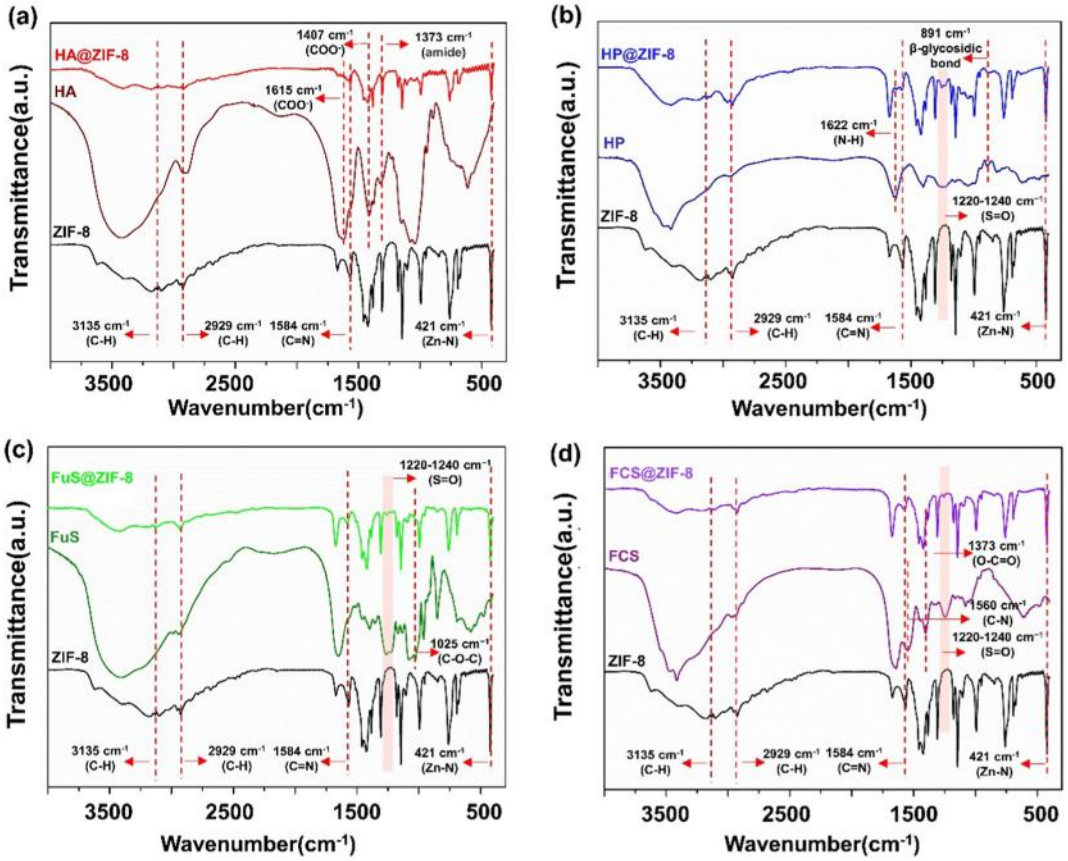

Fig. 4. The FTIR spectra of (a) ZIF-8, HA and HA@ZIF-8, (b) ZIF-8, HP and HP@ZIF-8, (c) ZIF-8, FuS and FuS@ZIF-8 (d) ZIF-8, FCS and FCS@ZIF-8.

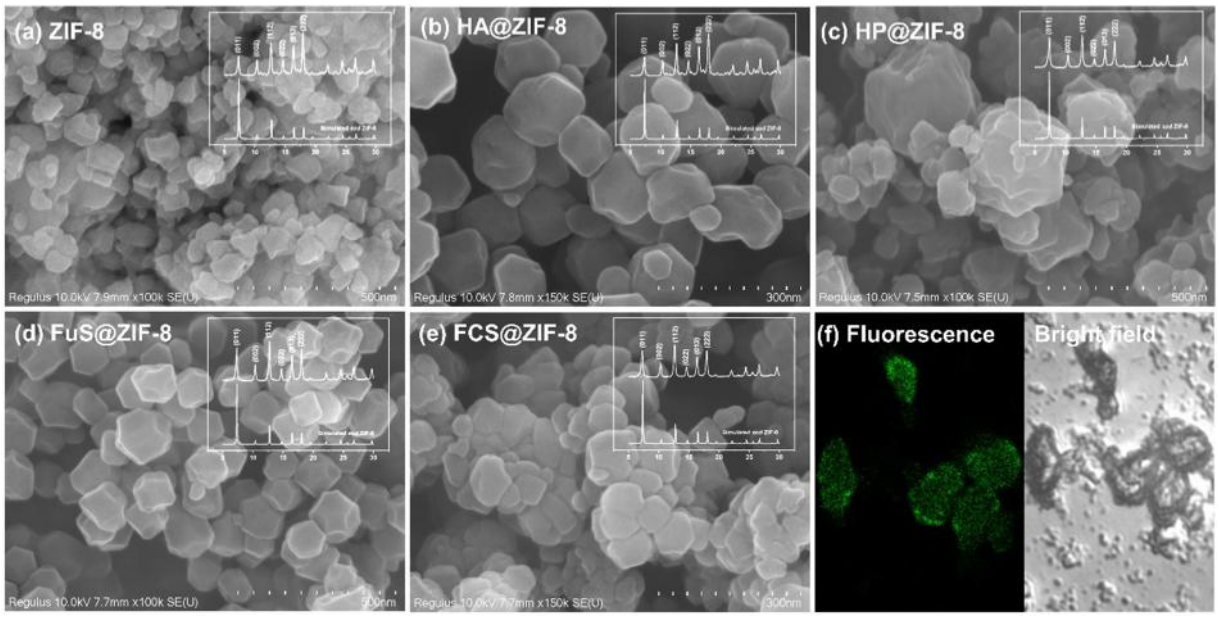

Fig. 5. SEM images and XRD patterns of (a) ZIF-8, (b) HA@ZIF-8, (c) HP@ZIF-8, (d) FuS@ZIF-8, (e) FCS@ZIF-8; (f) CLSM images showing the fluorescence and bright-field images of HA@ZIF-8.

polysaccharides were encapsulated during the growth process. A similar phenomenon has been reported in the previous reports [31,42].

N_2 adsorption-desorption isotherms and pore size distribution of ZIF-8 and polysaccharides@ZIF-8 biocomposites were shown in Fig. 6, and the textural parameters were summarized in Table S1. The isotherm of all exhibited type-1 isotherm (Fig. 6a). The steep increase in the adsorbed amount at low relative pressure revealed the presence of microporosity in the sample, and there was slight lag phenomenon in isotherm implying the existence of mesopores in the crystalline material. As shown in Fig. 6b, ZIF-8 and polysaccharides@ZIF-8 had a pore distribution ranging from micropores to mesopores, which further verified the coexisting of micro- and mesopores. In the morphology transformation of ZIF-8 growth, the nucleation rate plays a key role in crystal formation, which influenced by precursor concentration. The electrostatic interactions between polysaccharides and Zn^{2+} ions would cause a change of local concentrations of Zn^{2+} on the around of the polysaccharide that affected the morphologies of the final products. Obviously, the adsorption capacity of ZIF-8 was inferior to that of polysaccharides@ZIF-8 in the low-pressure region of $P/P0 < 0.01$ because of the lower BET surface area. The likely reason of diversity in adsorption capacity in four polysaccharides@ZIF-8 composite was structural difference in the crystals caused by different sugar structure as well, that impact gas diffusion/adsorption properties of the composite material.

3.3. The encapsulation efficiency and release test of polysaccharides@ZIF-8

The encapsulation efficiency (EE%) of each polysaccharides@ZIF-8 biocomposite was assessed using UV–vis spectroscopy (Fig. 7a). The HP@ZIF-8 presents the highest EE% reaching values above 95% and HA@ZIF-8 also shows excellent encapsulation effect (ca. 90%). The FCS@ZIF-8 displayed the lowest EE% (ca. 48%). In the case of ZIF-8, the biocomposites obtained from FuS present unsatisfactory EE% (ca. 70%). The difference in encapsulation efficiency can be attributed to electronegativity since negatively charged functional groups trigger the growth of biocomposites and can be employed for the encapsulation of polysaccharides in MOFs [43,44]. The amount of the polysaccharides encapsulated in ZIF-8 was confirmed by thermogravimetric analysis (TGA) (Fig. S3 and Table S2) and encapsulation efficiency were calculated as well.

Owing to the pH-sensitive property of ZIF-8, the drug-release profile studies were determined by quantifying the amount of polysaccharides delivered in a buffer of pH 5.6 and 7.4. The buffer was employed to

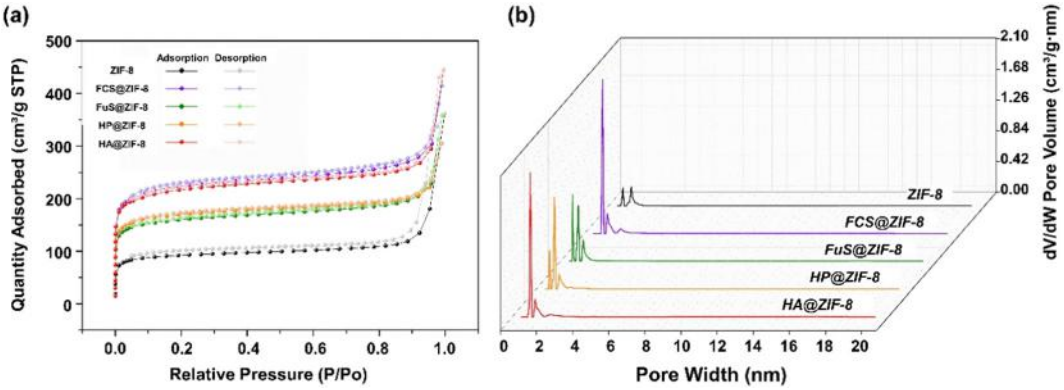

Fig. 6. (a) N_2 adsorption isotherms of ZIF-8, FCS@ZIF-8, FuS@ZIF-8, HP@ZIF-8, HA@ZIF-8; (b) the inset shows the BJH pore size distribution curve.

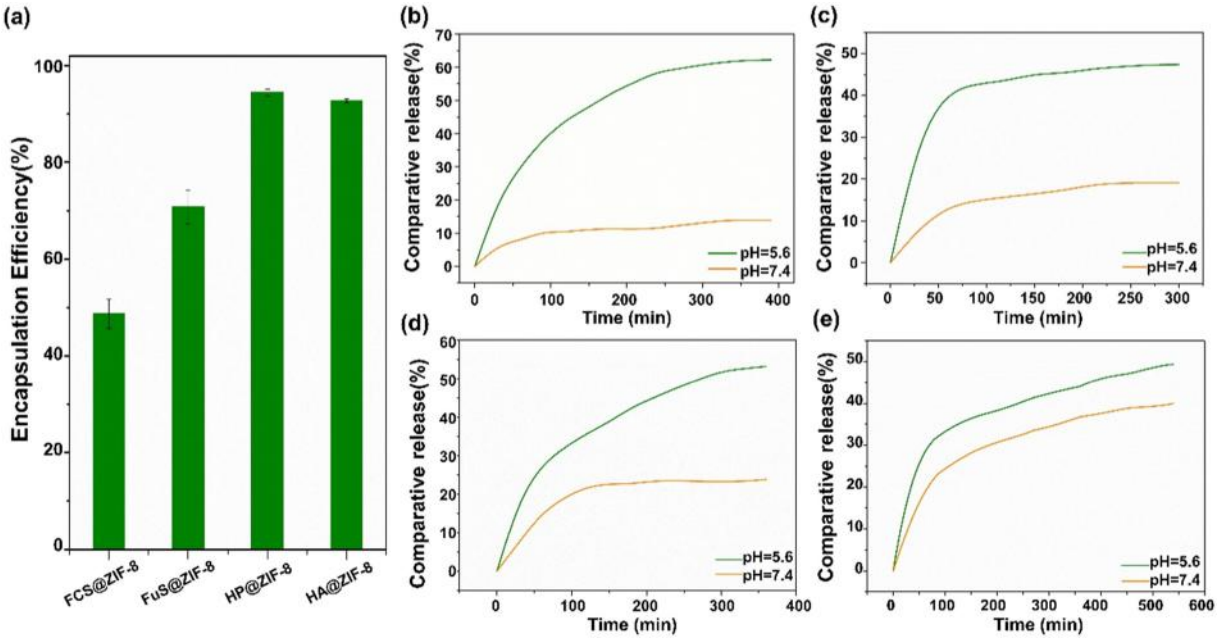

Fig. 7. (a) The encapsulation efficiency of the polysaccharides@ZIF-8. Comparative release profiles of the biocomposites: (b) HP@ZIF-8 (c) HA@ZIF-8, (d) FCS@ZIF-8, and (e) FuS@ZIF-8.

emulate the pH found in cancer cells and blood. All the release profiles presented an initial rapid release of the polysaccharides, followed by a slower sustained delivery. Nevertheless, each polysaccharides@ZIF-8 shows unique release behavior. The cumulative release rate of HP improved from 13% to 64%, when the pH value changed from 7.4 to 5.6 in 6 h (Fig. 7b). In the acidic environment, the coordination bond between 2-MIM and Zn^{2+} was destroyed, which resulted in a greater release of polysaccharides at pH 5.6 than at pH 7.4. HA in HA@ZIF-8 was released slowly in buffer at pH 7.4, showing less than 20% was released within 1.5 h, whereas a rapid release of approximately 45% during the 1.5 h was monitored in buffer at pH 5.6 (Fig. 7c). FCS loaded ZIF-8 exhibited a slow release at pH 7.4 with approximately 20% of the drug was released during 2 h (Fig. 7d). In contrast, the FCS release rate was markedly increased in an acidic buffer, consistent with the dissolution of ZIF-8 in the acidic environment. The accumulated FuS released was 48% and 39% in 6 h at pH 5.6 and pH 7.4 respectively. FuS@ZIF-8 exhibited fast release in the buffer of pH 5.6 and 7.4 at 1.5 h, then a relatively slow release of the dose was observed during the next 6 h. (Fig. 7e). These results suggest the disintegration of ZIF-8 NPs driven by the low pH can be exploited for polysaccharides release in acidic environments. As shown in Table 1, different MOFs have been employed to encapsulate various glycosaminoglycan therapeutics. Astria et al. investigated the role of mono-, di-, oligo-, and polysaccharides for the formation of carbohydrates@ZIF-8 effective encapsulation and release [44]. Velásquez-Hernández and coworkers successfully encapsulated glycosaminoglycan-based clinical drugs (heparin, hyaluronic acid, chondroitin sulfate, dermatan sulfate) in three different pH-responsive metal-azolate frameworks (ZIF-8, ZIF-90, and MAF-7) [31]. These MOFs not only have excellent encapsulation effect, but also show the protection of polysaccharides. Our work also proved that ZIF-8 had the ability to load and protect sugar. In addition, it exhibited a long-acting and sustainable release within 6 h, which is useful for solving the poor dose control of anticoagulant drugs and reducing side effects.

3.4. Anticoagulant activity of sulfated polysaccharides@ZIF-8 biocomposites

The anticoagulant activities were further evaluated by monitoring the kinetic curves of coagulation of standard rabbit plasma by measuring activated partial thromboplastin time (APTT) to test the possible alteration in the biotherapeutic properties of sulfated polysaccharides due to the encapsulation (Fig. 8). The optical density of the solution

Table 1
The encapsulation efficiency and release time of polysaccharides@MOFs biocomposites.

MOFs	Polysaccharides	Encapsulation efficiency (%)	Release time	Ref.
ZIF-8	Heparin, hyaluronan, chondroitin sulfate, dermatan sulfate	ca. 100%	Ranging from 40 min to 1 h	[31]
ZIF-90	Heparin, hyaluronan, chondroitin sulfate, dermatan sulfate	ca. 50%	Ranging from 50 min to 1.5 h	
MAF-7	Heparin, hyaluronan, chondroitin sulfate, dermatan sulfate	ca. 80%	The complete delivery being 30 min	
MIL-101(Fe)	heparin	ca. 90%	NA	[30]
ZIF-8	D-Glucose, D-xylose, Methyl-α-D-glucopyranoside, D-glucitol, Meglumine, *N*-acetyl-D-glucosamine, D-glucosamine hydrochloride, D-Gluconic acid-δ-lactone	100% (FITC-CM-dextran)	For the 10, 20, 40 mM EDTA solution, roughly 45, 30, 16 min is required to release 100% of FITC-CM-dextran.	[43]
ZIF-8	Heparin	95%	13% (pH 7.4) and 64% (pH 5.6) release after 1.5 h and in 6 h, respectively	This work
	Hyaluronic acid	90%	15% (pH 7.4) and 45% (pH 5.6) release after 1.5 h	
	Fucan sulfate	70%	39% (pH 7.4) and 48% (pH 5.6) release after 2 h and in 6 h, respectively	
	Fucosylated chondroitin sulfate	48%	20% (pH 7.4) and 55% (pH 5.6) release after 6 h	

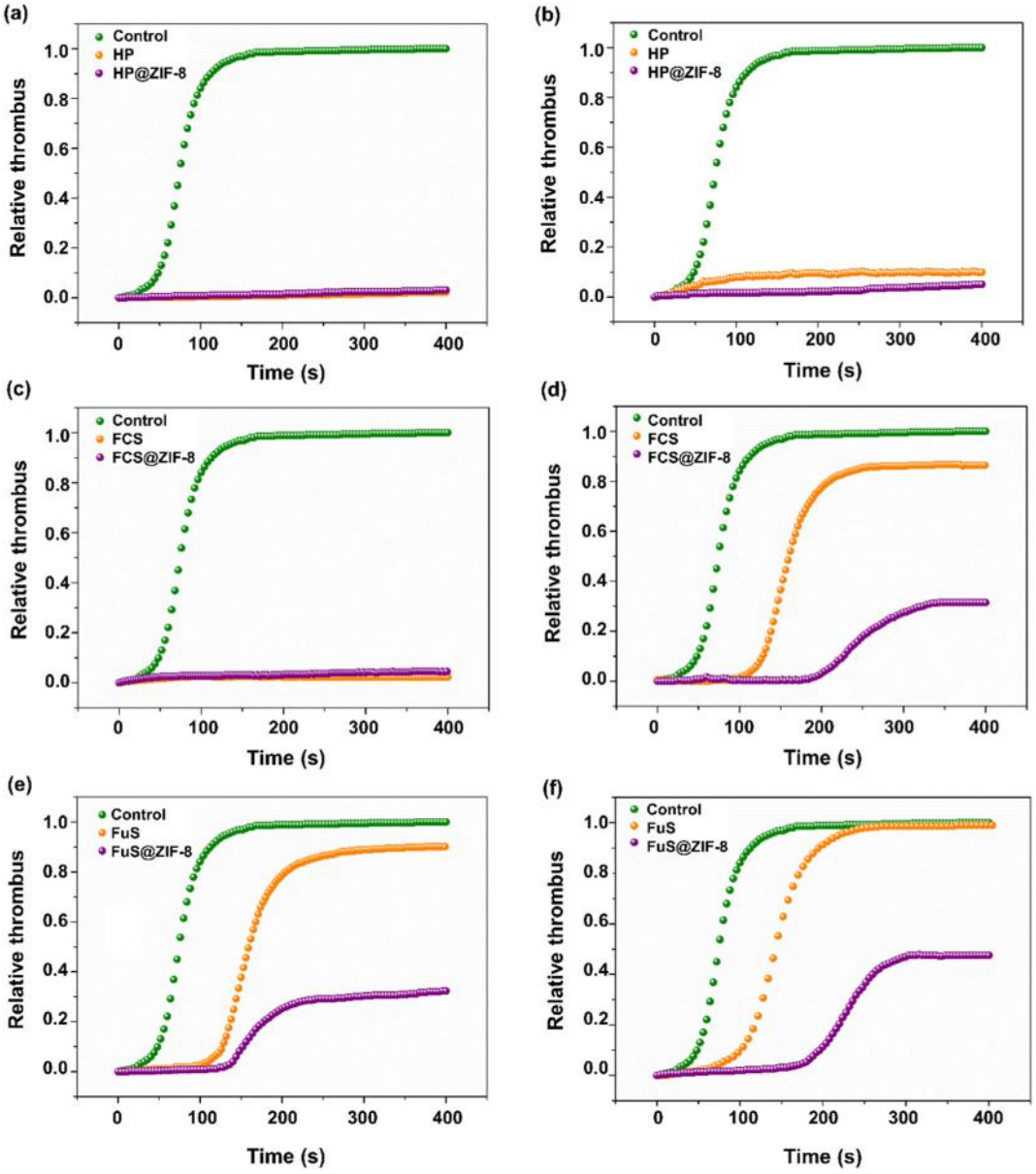

Fig. 8. The anticoagulant activity of (a) HP, HP@ZIF-8, (c) FCS, FCS@ZIF-8, (e) FuS, FuS@ZIF-8; The anticoagulant activity of (b) HP, HP@ZIF-8, (d) FCS, FCS@ZIF-8, (f) FuS, FuS@ZIF-8 after being exposed to pH 5.6 buffer for 6 h.

increased due to the conversion of fibrinogen to fibrin. APTT value is 72 s for control plasma. The data show that no detectable clot was found for as long as 400 s after the addition of free both sulfated polysaccharides and polysaccharides@ZIF-8 biocomposites, which shows the anticoagulant activity of the HP@ZIF-8 and FCS@ZIF-8 was almost as high as that of the free heparin and FCS respectively (Fig. 8a and c). The anticoagulant activity of FuS@ZIF-8 was less than FuS (Fig. 8e). The nature of the polysaccharide and polysaccharide-ZIF-8 interaction may affect the anticoagulant activity of the biocomposites. Sulfated polysaccharides@ZIF-8 biocomposites and the free sulfated polysaccharides were exposed to acidic buffer (pH 5.6) for 6 h at 37 °C to test the protective effect of ZIF-8 on those sulfated polysaccharides. Subsequently, the sulfated polysaccharides@ZIF-8 biocomposites were recovered and the anticoagulant activity was determined using APTT assay and compared with the activity of unprotected sulfated polysaccharides exposed to the same conditions. The relative thrombus of HP@ZIF-8 being exposed was close to untreated HP and HP@ZIF-8 (APTT value>400 s), but the optical density of the treated free HP increased (Fig. 8a and b), which indicates that ZIF-8 shell can protect polysaccharides from the unfavorable environment while maintaining the anticoagulant activity of the polysaccharides. The protective effect of ZIF-8 on FCS is also confirmed in Fig. 8d, where the optical density of the free FCS treated with pH 5.6 buffer increased faster than FCS@ZIF-8. The reason could be the acidic environment causes the cleaving of sulfated fucose branching leading to FCS losing potency. The anticoagulant activity of FCS and FCS@ZIF-8 both has decreased, but due to the protective effect, FCS@ZIF-8 shows a lower relative thrombotic value. It was found that after being exposed to pH 5.6 buffer for 6 h, FuS@ZIF-8 exhibited better anticoagulant activity than unprotected FuS (Fig. 8f), which was ascribed to the two reason: 1) The difference of sulfated polysaccharides. The diversity of sulfate substitution and sulfated fucose branches affect the anticoagulant activity of various sulfated polysaccharides, and the interaction between polysaccharides and ZIF-8 could further cause differences in anticoagulant behavior of polysaccharide; 2) Shielding effect of the ZIF-8. Compared with the neutral environment, the shielding effect of the ZIF-8 protects the sulfated polysaccharides from being

damaged, maintaining their stability and activity in acidic conditions. Meanwhile, the structure of ZIF-8 was loosened in the acidic conditions because of the dual role of H^+ and phosphates; thus, more FuS was released to the solution which caused better anticoagulant activity [45,46].

4. Conclusion

In this study, ZIF-8 was used to design pH-responsive carriers for the encapsulation and release of polysaccharides including heparin (HP), fucan sulfate (FuS), fucosylated chondroitin sulfate (FCS), and hyaluronic acid (HA). We examined the encapsulation of four polysaccharides: the loading capacity of the four polysaccharides is 95% (HP), 90% (HA), 48% (FCS), and 70% (FuS), respectively, and the release time varied from 1 h to 6 h. A controlled and sustained release of the biomolecule is required to reduce the systemic side effects associated with high drug concentrations, polysaccharides@ZIF-8 biocomposites is a desirable alternative. In rabbit plasma, these biocomposites retained antithrombotic activity and the ZIF-8 effectively protects the sulfated polysaccharide from degradation and prolonged shelf-life of the anticoagulants from the unfavorable environment. It is interesting to find that the anticoagulant activity of the FuS@ZIF-8 was higher than the FuS. We suggest that this phenomenon can be attributed to the different interaction of polysaccharide-ZIF-8 and the nature of the various polysaccharides, and the discovery of the underlying mechanism will be our future focus. In summary, the structure of polysaccharides is of great significance to their biological functions, and this polysaccharides@ZIF-8 design promises a potential delivery strategy for both sulfated polysaccharides self-protecting and more long-term release. Despite remarkable achievements made in drug delivery, several challenges remain to be solved for MOFs. For instance, molecules incorporated by surface adsorption and pore encapsulation tend to leak gradually owing to weak interaction forces. However, covalent binding provides stronger interactions that may influence the activity of functional molecules. On the other hand, the kinetics of drug loading and release, in vivo toxicity, and degradation mechanism of MOF nanoparticles are still under study. In conclusion, MOFs are a class of promising candidates in drug delivery. In the future, efforts should be focused on overcoming the noted challenges to fully realize the potential of drug delivery systems.

CRediT authorship contribution statement

Xun Lv: Conceptualization, Methodology, Software. **Jie Zheng**: Data curation, Writing- Original draft preparation. **Yin Chen**: Visualization, Investigation. **Robert J. Linhardte**, **Xing Zhang**: Supervision. **Yuan Ji**: Software, Validation. **Bingzhi Li**, **Xing Zhang**: Writing- Reviewing and Editing.

Declaration of competing interest

There are no conflicts to declare.

Acknowledgements

The authors were supported in part by grants from the National Natural Science Foundation of China (22007049) and the Natural Science Foundation of Jiangsu Province (BK20200728 and BK20200718) and Natural Science Research Project of Jiangsu Higher Education Institutions (19KJB150013).

Appendix A. Supplementary data

Supplementary data to this article can be found online at https://doi.org/10.1016/j.ijbiomac.2021.05.007.

References

[1] L. Lin, Y. Yu, F. Zhang, K. Xia, X. Zhang, R.J. Linhardt, Bottom-up and top-down profiling of pentosan polysulfate, Analyst 144 (2019) 4781–4786, https://doi.org/10.1039/C9AN01006H.
[2] R. Cao, Y. Lee, S. You, Water soluble sulfated-fucans with immune-enhancing properties from *Ecklonia cava*, Int. J. Biol. Macromol. 67 (2014) 303–311, https://doi.org/10.1016/j.ijbiomac.2014.03.019.
[3] J. Wang, A. Bao, X. Meng, H. Guo, Y. Zhang, Y. Zhao, W. Kong, J. Liang, J. Yao, J. Zhang, An efficient approach to prepare sulfated polysaccharide and evaluation of antitumor activities in vitro, Carbohydr. Polym. 184 (2018) 366–375, https://doi.org/10.1016/j.carbpol.2017.12.065.
[4] F. Yuan, Z. Gao, W. Liu, H. Li, Y. Zhang, Y. Feng, X. Song, W. Wang, J. Zhang, C. Huang, L. Jia, Characterization, antioxidant, anti-aging and organ protective effects of sulfated polysaccharides from flammulina velutipes, Molecules 24 (2019) 3517, https://doi.org/10.3390/molecules24193517.
[5] F.D.d.S. Chagas, G.C. Lima, V.I.N. Santos, L.E.C. Costa, W.M. Sousa, V.G. Sombra, D.F. Araújo, F.C.N. Barros, E. Marinho-Soriano, J.P.d.A. Feitosa, R.C.M.d. Paula, M.G. Pereira, A.L.P. Freitasa, Sulfated polysaccharide from the red algae gelidiella acerosa: anticoagulant, antiplatelet and antithrombotic effects, Int. J. Biol. Macromol. 159 (2020) 415–421, https://doi.org/10.1016/j.ijbiomac.2020.05.012.
[6] P.S. Kwon, H. Oh, S.-J. Kwon, W. Jin, F. Zhang, K. Fraser, J.J. Hong, R.J. Linhardt, J.S. Dordick, Sulfated polysaccharides effectively inhibit SARS-CoV-2 in vitro, Cell Discov. 6 (2020), 50, https://doi.org/10.1038/s41421-020-00192-8.
[7] E.I. Oduah, R.J. Linhardt, S.T. Sharfstein, Heparin: past, present, and future, Pharmaceuticals 9 (2016) 38, https://doi.org/10.3390/ph9030038.
[8] A.R. Neves, M. Correia-da-Silva, E. Sousa, M. Pinto, Strategies to overcome heparins' low oral bioavailability, pharmaceuticals 9 (2016) 37, https://doi.org/10.3390/ph9030037.
[9] N.S. Gandhi, R.L. Mancera, Heparin/heparan sulphate-based drugs, Drug Discov. Today 15 (2010) 1058–1069, https://doi.org/10.1016/j.drudis.2010.10.009.
[10] X. Zhang, L. Lin, H. Huang, R.J. Linhardt, Chemoenzymatic synthesis of glycosaminoglycans, Acc. Chem. Res. 53 (2020) 335–346, https://doi.org/10.1021/acs.accounts.9b00420.
[11] X. Zhang, X. Han, K. Xia, Y. Xu, Y. Yang, K. Oshima, S.M. Haeger, M.J. Perez, S.A. McMurtry, J.A. Hippensteel, J.A. Ford, P.S. Herson, J. Liu, E.P. Schmidt, R.J. Linhardt, Circulating heparin oligosaccharides rapidly target the hippocampus in sepsis, potentially impacting cognitive functions, Proc. Natl. Acad. Sci. U. S. A. 116 (2019) 9208–9213, https://doi.org/10.1073/pnas.1902227116.
[12] B. Pradhan, S. Patra, R. Nayak, C. Behera, S.R. Dash, S. Nayak, B.B. Sahu, S.K. Bhutia, M. Jena, Multifunctional role of fucoidan, sulfated polysaccharides in human health and disease: a journey under the sea in pursuit of potent therapeutic agents, Int. J. Biol. Macromol. 164 (2020) 4263–4278, https://doi.org/10.1016/j.ijbiomac.2020.09.019.
[13] P. Myron, S. Siddiquee, S.A. Azad, Fucosylated chondroitin sulfate diversity in sea cucumbers: a review, Carbohydr. Polym. 112 (2014) 173–178, https://doi.org/10.1016/j.carbpol.2014.05.091.
[14] X. Zhang, W. Yao, X. Xu, H. Sun, J. Zhao, X. Meng, M. Wu, Z. Li, Synthesis of fucosylated chondroitin sulfate glycoclusters: a robust route to new anticoagulant agents, Chem. Eur. J. 24 (2018) 1694–1700, https://doi.org/10.1002/chem.201705177.
[15] L. Yan, M. Zhu, D. Wang, W. Tao, D. Liu, F. Zhang, R.J. Linhardt, X. Ye, S. Chen, Oral aministration of fucosylated chondroitin sulfate oligomers in gastro-resistant microcapsules exhibits a safe antithrombotic activity, Thromb. Haemost. 121 (2021) 015–026, https://doi.org/10.1055/s-0040-1714738.
[16] P.A.S. Mourão, M.A.M. Guimarães, B. Mulloy, S. Thomas, E. Gray, Antithrombotic activity of a fucosylated chondroitin sulphate from echinoderm: sulphated fucose branches on the polysaccharide account for its antithrombotic action, Br. J. Haemato. 101 (1998) 647–652, https://doi.org/10.1046/j.1365-2141.1998.00769.x.
[17] Y.B. Lin, Y. Yang, Y.J. Zhao, F. Gao, X. Guo, M.H. Yang, Q.X. Hong, Z.M. Yang, J. Dai, H.J. Pan, Incorporation of heparin/BMP2 complex on GOCS-modified magnesium alloy to synergistically improve corrosion resistance, anticoagulation, and osteogenesis, J. Mater. Sci-Mater. M. 32 (2019) 24, https://doi.org/10.1007/s10856-021-06497-8.
[18] C. Li, M. Zhang, X. Liu, W. Zhao, C. Zhao, Immobilization of heparin-mimetic biomacromolecules on Fe_3O_4 nanoparticles as magnetic anticoagulant via mussel-inspired coating, Mater. Sci. Eng. C-Mater. 109 (2020), 110516, https://doi.org/10.1016/j.msec.2019.110516.
[19] M. Wan, W. Qian, W. Lin, Y. Zhou, J. Zhu, Multiple functionalization of SBA-15 mesoporous silica in one-pot: fabricating an aluminum-containing plugged composite for sustained heparin release, J. Mater. Chem. B (32) (2013) 3897–3905, https://doi.org/10.1039/C3TB20425A.
[20] B.S. Caldasa, C.S. Nunesa, M.R. Panicea, D.B. Scariot, C.V. Nakamura, E.C. Muniz, Manufacturing micro/nano chitosan/chondroitin sulfate curcumin-loaded hydrogel in ionic liquid: a new biomaterial effective against cancer cells, Int. J. Biol. Macromol. 180 (2021) 88–96, https://doi.org/10.1016/j.ijbiomac.2021.02.194.
[21] Y. Liu, H. Lv, L. Ren, G. Xue, Y. Wang, Improving the moisturizing properties of collagen film by surface grafting of chondroitin sulfate for corneal tissue engineering, J. Biomat. Sci-Polym. E. 27 (2016) 758–772, https://doi.org/10.1080/09205063.2016.1160561.
[22] J. Cui, S. Ren, B. Sun, S. Jia, Optimization protocols and improved strategies for metal-organic frameworks for immobilizing enzymes: current development and future challenges, Coord. Chem. Rev. 370 (2018) 22–41, https://doi.org/10.1016/j.ccr.2018.05.004.
[23] B. Sun, M. Bilal, S. Jia, Y. Jiang, J. Cui, Design and bio-applications of biological metal-organic frameworks, Korean J. Chem. Eng. 36 (2019) 1949–1964, https://doi.org/10.1007/s11814-019-0394-8.

[24] Y. Feng, H. Hu, Z. Wang, Y. Du, L. Zhong, C. Zhang, Y. Jiang, S. Jia, J. Cui, Three-dimensional ordered magnetic macroporous metal-organic frameworks for enzyme immobilization, J. Colloid Interface Sci. 590 (2021) 436–445, https://doi.org/10.1016/j.jcis.2021.01.078.
[25] Y. Sun, L. Zheng, Y. Yang, X. Qian, Ti Fu, X. Li, Z. Yang, H. Yan, C. Cui, W. Tan, Metal-organic framework nanocarriers for drug delivery in biomedical applications, Nano-Micro Lett. 12 (2020), 103, https://doi.org/10.1007/s40820-020-00423-3.
[26] Y. Feng, L. Zhong, M. Bilal, Z. Tan, Y. Hou, S. Jia, J. Cui, Enzymes@ZIF-8 nanocomposites with protection nanocoating: stability and acid-resistant evaluation, Polymers 11 (2019) 27, https://doi.org/10.3390/polym11010027.
[27] , [18]. H.N. Abdelhamid, Biointerface between ZIF-8 and biomolecules and their applications, Biointer. Res. Appl. Chem. 11 (2021) 8283–8297, https://doi.org/10.33263/BRIAC111.82838297.
[28] J. Li, M. Qiao, Y. Ji, L. Lin, X. Zhang, R.J. Linhardt, Chemical, enzymatic and biological synthesis of hyaluronic acids, Int. J. Biol. Macromol. 152 (2020) 199–206, https://doi.org/10.1016/j.ijbiomac.2020.02.214.
[29] W. He, H. Sun, L. Su, D. Zhou, X. Zhang, S. Deng, Y. Chen, Structure and anticoagulant activity of a sulfated fucan from the sea cucumber *Acaudina leucoprocta*, Int. J. Biol. Macromol. 164 (2020) 87–94, https://doi.org/10.1016/j.ijbiomac.2020.07.080.
[30] V.V. Vinogradov, A.S. Drozdov, L.R. Mingabudinova, E.M. Shabanova, N.O. Kolchina, E.I. Anastasova, A.A. Markova, A.A. Shtil, V.A. Milichko, G.L. Starova, R.L.M. Precker, A.V. Vinogradov, E. Hey-Hawkins, E.A. Pidko, Composites based on heparin and MIL-101 (Fe): the drug releasing depot for anticoagulant therapy and advanced medical nanofabrication, J. Mater. Chem. B 6 (2018) 2450–2459, https://doi.org/10.1039/C8TB00072G.
[31] M.d.J. Velásquez-Hernández, E. Astria, S. Winkler, W. Liang, H. Wiltsche, A. Poddar, R. Shukla, G. Prestwich, J. Paderi, P. Salcedo-Abraira, H. Amenitsch, P. Horcajada, C.J. Doonan, P. Falcaro, Modulation of metal-azolate frameworks for the tunable release of encapsulated glycosaminoglycans, Chem. Sci. 11 (2020) 10835–10843, https://doi.org/10.1039/D0SC01204A.
[32] M. DuBois, K.A. Gilles, J.K. Hamilton, P.A. Rebers, F. Smith, Colorimetric method for determination of sugars and related substances, Anal. Chem. 28 (1956) 350–356, https://doi.org/10.1021/ac60111a017.
[33] A.D. Katsenis, A. Puškarić, V. Štrukil, C. Mottillo, P.A. Julie, K. Užarević, M.-H. Pham, T.-O. Do, S.A.J. Kimber, P. Lazić, O. Magdysyuk, R.E. Dinnebier, I. Halasz, T. Friščić, In situ X-ray diffraction monitoring of a mechanochemical reaction reveals a unique topology metal-organic framework, Nat. Commun. 6 (2015) 6662, https://doi.org/10.1038/ncomms7662.
[34] Y. Lo, C. Lam, C. Chang, A. Yang, D. Kang, Polymorphism/pseudopolymorphism of metalorganic frameworks composed of zinc(II) and 2methylimidazole: synthesis, stability, and application in gas storage, RSC Adv. (92) (2016) 89148–89156, https://doi.org/10.1039/C6RA19437K.
[35] P. Li, Y. Maeda, Q. Xu, Top-down fabrication of crystalline metal-organic framework nanosheets, Chem. Commun. 47 (2011) 8436–8438, https://doi.org/10.1039/C1CC12510A.
[36] Y. Hu, H. Kazemian, S. Rohani, Y. Huang, Y. Song, In situ high pressure study of ZIF-8 by FTIR spectroscopy, Chem. Commun. 47 (2011) 12694–12696, https://doi.org/10.1039/C1CC15525C.
[37] Y. Liu, Z. Li, S. Zou, C. Lu, Y. Xiao, H. Bai, X. Zhang, H. Mu, X. Zhang, J. Duan, Hyaluronic acid-coated ZIF-8 for the treatment of pneumonia caused by methicillin-resistant *Staphylococcus aureus*, Int. J. Biol. Macromol. 155 (2020) 103–109, https://doi.org/10.1016/j.ijbiomac.2020.03.187.
[38] C.V. García, N.F. Fernández, M.D. Torres, M.J.L. Vázquez, F.J. Blanco, H. Domínguez, R.M. Faíldeac, Study of fucoidans as natural biomolecules for therapeutical applications in osteoarthritis, Carbohydr. Polym. 258 (2021) 117692, https://doi.org/10.1016/j.carbpol.2021.117692.
[39] M.B. Mansour, R. Balt, V. Ollivier, H.B. Jannet, F. Chaubet, R.M. Maaroufi, Characterization and anticoagulant activity of a fucosylated chondroitin sulfate with unusually procoagulant effect from sea cucumber, Carbohydr. Polym. 174 (2017) 760–771, https://doi.org/10.1016/j.carbpol.2017.06.128.
[40] H. Zheng, Y. Zhang, L. Liu, W. Wan, P. Guo, A.M. Nyström, X. Zou, One-pot synthesis of metal organic frameworks with encapsulated target molecules and their applications for controlled drug delivery, J. Am. Chem. Soc. 138 (2016) 962–968, https://doi.org/10.1021/jacs.5b11720.
[41] K. Kida, M. Okita, K. Fujita, S. Tanaka, Y. Miyake, Formation of high crystalline ZIF-8 in an aqueous solution, Crystengcomm 15 (2013) 1794–1801, https://doi.org/10.1039/C2CE26847G.
[42] W. Liang, H. Xu, F. Carraro, N.K. Maddigan, Qi. Li, S.G. Bell, D.M. Huang, A. Tarzia, M.B. Solomon, H. Amenitsch, L. Vaccari, C.J. Sumby, P. Falcaro, C.J. Doonan, Enhanced activity of enzymes encapsulated in hydrophilic metal-organic frameworks, J. Am. Chem. Soc. 141 (2019) 2348–2355, https://doi.org/10.1021/jacs.8b10302.
[43] N.K. Maddigan, A. Tarzia, D.M. Huang, C.J. Sumby, S.G. Bell, P. Falcaro, C.J. Doonan, Protein surface functionalisation as a general strategy for facilitating biomimetic mineralisation of ZIF-8, Chem. Sci. 9 (2018) 4217–4223, https://doi.org/10.1039/C8SC00825F.
[44] E. Astria, M. Thonhofer, R. Ricco, W. Liang, A. Chemelli, A. Tarzia, K. Alt, C.E. Hagemeyer, J. Rattenberger, H. Schroettner, T. Wrodnigg, H. Amenitsch, D.M. Huang, C.J. Doonan, P. Falcaro, Carbohydrates@MOFs, Mater. Horiz. 6 (2019) 969–977, https://doi.org/10.1039/C8MH01611A.
[45] M.d.J.V. Hernández, R. Ricco, F. Carraro, F.T. Limpoco, M.Li. Moreau, E. Leitner, H. Wiltsche, J. Rattenberger, H. Schröttner, P. Frühwirt, E.M. Stadler, G. Gescheidt, H. Amenitsch, C.J. Doonan, P. Falcaro, Degradation of ZIF-8 in phosphate buffered saline media, Crystengcomm 21 (2019) 4538–4544, https://doi.org/10.1039/C9CE00757A.
[46] J. Yan, et al., Mineralization of pH-sensitive doxorubicin prodrug in ZIF-8 to enable targeted delivery to solid tumors, Anal. Chem. 92 (2020) 11453–11461, https://doi.org/10.1021/acs.analchem.0c02599.